Green Tea Polyphenol Epigallocatechin-3-Gallate Suppresses Collagen Production and Proliferation in Keloid Fibroblasts via Inhibition of the STAT3-Signaling Pathway

Gyuman Park[1], Byung Sun Yoon[2], Jai-Hee Moon[2], Bona Kim[2], Eun Kyoung Jun[2], Sejong Oh[3], Hyunggee Kim[2], Hea Joon Song[1], Joo Young Noh[4], ChilHwan Oh[2] and Seungkwon You[2]

Keloids are benign skin tumors characterized by collagen accumulation and hyperproliferation of fibroblasts. To find an effective therapy for keloids, we explored the pharmacological potential of (−)-epigallocatechin-3-gallate (EGCG), a widely investigated tumor-preventive agent. When applied to normal and keloid fibroblasts (KFs) *in vitro*, proliferation and migration of KFs were more strongly suppressed by EGCG than normal fibroblast proliferation and migration (IC_{50}: 54.4 μM (keloid fibroblast (KF)) *versus* 63.0 μM (NF)). The level of Smad2/3, signal transducer and activator of transcription-3 (STAT3), and p38 phosphorylation is more enhanced in KFs, and EGCG inhibited phosphorylation of phosphatidylinositol-3-kinase (PI3K), extracellular signal-regulated protein kinase 1/2 (ERK1/2), and STAT3 (Tyr705 and Ser727). To evaluate the contribution of these pathways to keloid pathology, we treated KFs with specific inhibitors for PI3K, ERK1/2, or STAT3. Although a PI3K inhibitor significantly suppressed proliferation, PI3K and MEK/ERK inhibitors had a minor effect on migration and collagen production. However, a JAK2/STAT3 inhibitor and a STAT3 siRNA strongly suppressed proliferation, migration, and collagen production by KFs. We also found that treatment with EGCG suppressed growth and collagen production in the *in vivo* keloid model. This study demonstrates that EGCG suppresses the pathological characteristics of keloids through inhibition of the STAT3-signaling pathway. We propose that EGCG has potential in the treatment and prevention of keloids.

Journal of Investigative Dermatology (2008) **128,** 2429–2441; doi:10.1038/jid.2008.103; published online 8 May 2008

INTRODUCTION

Keloids are benign cutaneous tumors, which extend beyond wound margins (Rekha, 2004). Their pathology is distinguishable from that of normal skin by the substantial deposition of collagen in the dermis, resulting in imbalanced production and aggregation of the extracellular matrix (Marneros and Krieg, 2004). Although there are no known cases of keloids transforming into malignant tumors, they behave like benign dermal fibroproliferative tumors, as they continue to grow and extend beyond the confines of the original wound margins and do not spontaneously regress (Ehrlich *et al.*, 1994). The difficulty in treating keloids is evidenced by the large number of modalities of treatment (Al-Attar *et al.*, 2006). The most common therapeutic option for keloids are intra-lesional injections of dexamethasone (Marneros and Krieg, 2004; Rekha, 2004; Mutalik, 2005), but these injections are often unsuccessful (Al-Attar *et al.*, 2006).

There are several hypotheses as to the cause of keloid formation, including altered growth-factor regulation, immune dysfunction, aberrant collagen turnover, sebum or sebocytes as self-antigens, and altered mechanics (Al-Attar *et al.*, 2006). No single unifying factor responsible for keloid formation has been identified. Although the exact pathophysiology of keloid formation is unclear, previous studies have focused on investigating abnormal increases in growth factors and cytokines, such as transforming growth factor-α and transforming growth factor-β, vascular endothelial growth

[1]*Department of Dermatology, School of Medicine, Korea University, Seoul, Korea;* [2]*Division of Biotechnology and Genetic Engineering, College of Life Sciences and Biotechnology, Korea University, Seoul, Korea;* [3]*Division of Animal Sciences, College of Agriculture and Life Sciences, Chonnam National University, Kwangju, Korea and* [4]*Department of Dermatology, Gachon University of Medicine and Science, Incheon, Korea*

Correspondence: Dr Seungkwon You, Division of Biotechnology and Genetic Engineering, College of Life Sciences and Biotechnology, Korea University, 1, 5-ka, Anam-dong, Sungbuk-Gu, Seoul 136-701, Korea.
E-mail: bioseung@korea.ac.kr or ChilHwan Oh, Research Institute for Skin Image, Department of Dermatology, School of Medicine, Korea University, 1, 5-ka, Anam-dong, Sungbuk-Gu, Seoul 136-701, Korea.
E-mail: choh@korea.ac.kr

Abbreviations: AKT, acutely transforming retrovirus AKT8 in rodent T-cell lymphoma; EGCG, (−)-epigallocatechin-3-gallate; ERK1/2, extracellular signal-regulated protein kinase 1/2; FBS, fetal bovine serum; GSK, glycogen synthase kinase; JNK, c-Jun NH_2-terminal kinase; KF, keloid fibroblast; MAPK, mitogen-activated protein kinase; NF, normal fibroblast; PBS, phosphate-buffered saline; PI3K, phosphatidylinositol-3-kinase; siRNA, small interfering RNA; Smad, Sma- and Mad-related proteins; STAT3, signal transducer and activator of transcription-3; TUNEL, terminal deoxynucleotide transferase-mediated dUTP nick-end labeling; VEGF, vascular endothelial growth factor

Received 12 October 2007; revised 25 February 2008; accepted 7 March 2008; published online 8 May 2008

factor (VEGF), insulin growth factor, IL-6, and tumor-necrosis factors, which are likely to alter the wound healing process (Kelly, 2004). Although signaling by these growth factors and cytokines is mediated by different receptors, they share common intracellular effectors such as extracellular signal-regulated protein kinase 1/2 (ERK1/2), p38 mitogen-activated protein kinase (MAPK), Sma- and Mad-related proteins (Smads), signal transducer and activator of transcription-3 (STAT3), and phosphatidylinositol-3-kinase (PI3K). For example, TGF-β activates members of the Smad family, and TGF-β expression is transcriptionally regulated by the p38, MEK/ERK, and c-Jun NH_2-terminal kinase (JNK) pathways (Al-Attar *et al.*, 2006; Wang *et al.*, 2006; Xia *et al.*, 2006). Thus, many research groups have suggested modulation of these signaling mediators to treat keloids. Many previous studied demonstrated that suppression of Smad3, PI3K, ERK, and STAT3 pathways is sufficient to inhibit extracellular matrix production in keloids (Lim *et al.*, 2003, 2006; Phan *et al.*, 2004; Wu *et al.*, 2004; Zhang *et al.*, 2004; Xia *et al.*, 2006).

Green tea is one of the most widely consumed beverages in Asia and represents a promising dietary source of chemopreventive and chemoprotective phytochemicals (Dreosti *et al.*, 1997). Many epidemiological studies have shown a protective effect of green tea against the development of various types of cancers. Epigallocatechin-3-gallate (EGCG) is one of the most abundant polyphenols present in green tea (Kada *et al.*, 1985). The chemopreventive and selective antitumor effects of EGCG have been studied extensively using animal carcinogenesis models as well as several types of cultured cancer cell lines (Ahn *et al.*, 1999; Surh *et al.*, 2001; DiPaola, 2002; Chen *et al.*, 2003; Gupta *et al.*, 2003). EGCG has also been shown to modulate multiple signal transduction pathways, including those mediated by PI3K, MAPKs (ERK, p38 MAPK, and JNK), STAT3, Smad2/3, and nuclear factor-κB, which all play significant roles in tumorigenesis (Ahn *et al.*, 1999; Surh *et al.*, 2001; DiPaola, 2002; Chen *et al.*, 2003; Gupta *et al.*, 2003).

In this study, we tested the therapeutic potential of the green tea polyphenol EGCG for treatment of keloids. Because of the tumor-suppressive ability of EGCG, we postulated that EGCG can reduce skin defects associated with keloids. We found that EGCG treatment suppressed proliferation and migration of normal and keloid fibroblasts (KFs) *in vitro*, but it suppressed the proliferation and migration of KFs more than that of normal fibroblasts (NFs). To determine the inhibitory mechanism of EGCG, we compared the signaling responses of NFs and KFs. We found that phosphorylation of Smad2/3, STAT3, and p38 is enhanced in KFs, and the PI3K, MEK/ERK, and STAT3 signaling pathways are inhibited by EGCG. Using specific inhibitors and small interfering RNA (siRNA) technique, we found that STAT3 is an important signaling mediator for keloid pathology. Finally, we evaluated the pharmacological potential of EGCG *in vivo* using a keloid model. Treatment with EGCG suppressed growth and collagen production of keloid nodules. Our findings suggest that EGCG inhibits the pathological characteristics of keloids by suppressing STAT3 signaling. We suggest that EGCG has potential as a therapeutic and preventive agent for keloids.

RESULTS

EGCG strongly inhibits KF proliferation

To explore the potential of EGCG as a keloid treatment agent, we determined its effects on proliferation of normal and KFs. Various doses of EGCG were administered to NFs and KFs in culture and the effect on growth was determined by crystal violet staining (Figure 1a and c). As previously described, KFs grew faster than NFs (Nowak *et al.*, 2000; Luo *et al.*, 2001; Lim *et al.*, 2006). After 5 days in culture, KFs were almost confluent, but continued to grow well past confluence. However, proliferation of both NFs and KFs was reduced by EGCG at doses of 25–100 μM. Interestingly, proliferation of KFs was more strongly suppressed by EGCG than was NF proliferation (IC_{50}, 54.4 μM (KF) *versus* 63.0 μM (NF), on day 6). We also compared proliferation of NFs and KFs under low-serum and low-cell density conditions to examine whether EGCG suppressed abnormal growth of KFs. Under low-serum (0.2%) conditions, KFs proliferated more rapidly than NFs (Figure 1b). However, the enhanced proliferation of KFs was completely inhibited by 25 μM EGCG. In addition, under low-density culture conditions, KFs proliferated more rapidly and generated larger colonies than NFs, but the colony number of KFs was reduced by EGCG treatment (Figure 1d). These results indicate that EGCG more strongly inhibited proliferation of KFs than that of NFs under *in vitro* culture conditions.

EGCG induces cell-cycle arrest rather than an exit from the cell cycle in KFs

To determine the mechanism by which EGCG inhibits growth of KFs, we analyzed apoptosis, replicative senescence, and cell-cycle arrest in KFs in response to EGCG treatment. To identify apoptotic cells, we performed a terminal deoxynucleotide transferase-mediated dUTP nick-end labeling (TUNEL) assay following EGCG treatment. As shown in Figure 1e, EGCG treatment did not significantly alter the percentage of TUNEL-positive cells 2 days later. Moreover, the percentage of TUNEL-positive cells did not increase after 7 days of exposure to EGCG (data not shown). We examined whether EGCG administration was correlated with accumulation of cells possessing a sub-G_1/S DNA content, as a measure of apoptosis and necrosis, using flow cytometry. We found that after 2 days of EGCG treatment, there was no considerable increase in sub-G_1/S DNA content (Figure 1f; Figure S1a). In contrast, treatment with the anticancer drug adriamycin induced a large accumulation of cells possessing a sub-G_1/S DNA content (Figure 1f; Figure S1a). Furthermore, western blot analysis demonstrated that levels of the proactive and cleaved forms of PARP, caspase-3, and caspase-9, were not affected by treatment with EGCG for 1 day (Figure S1b).

We also investigated whether EGCG induces replicative senescence in KFs using senescence-associated β-galactosidase staining. After 2 days of incubation with EGCG, the percentage of senescence-associated β-galactosidase-positive cells remained unchanged (data not shown). These results

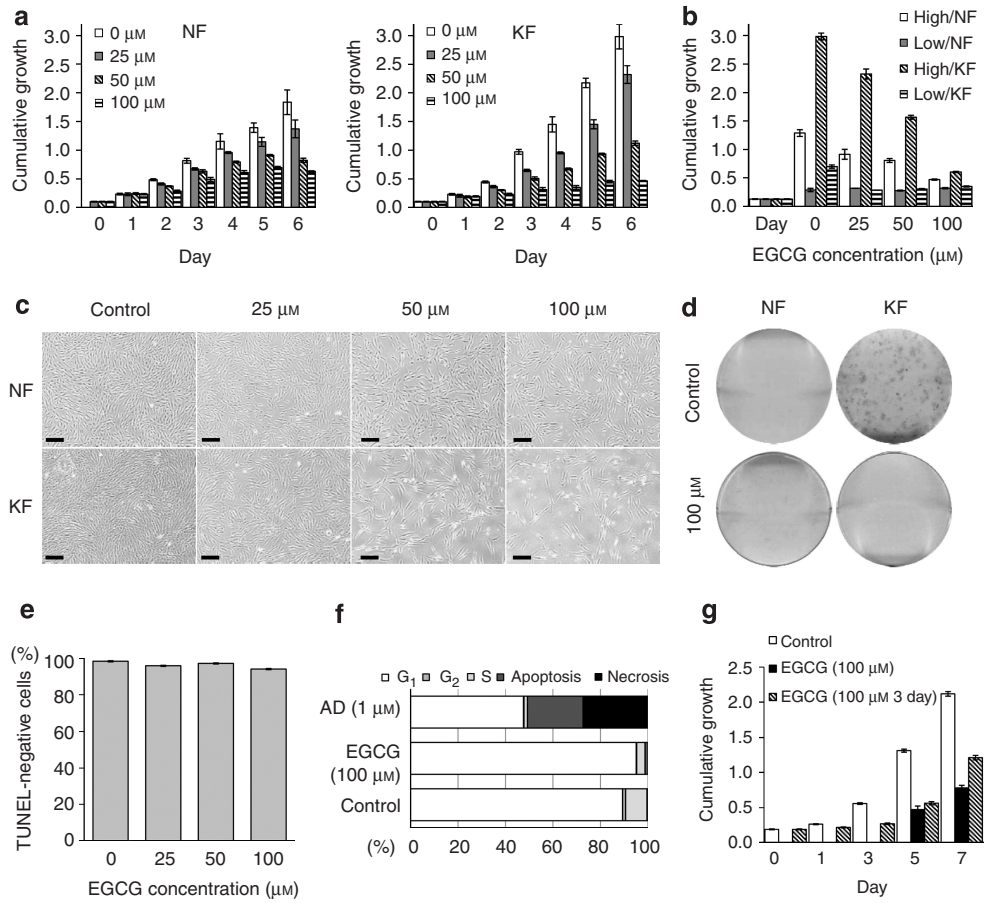

Figure 1. EGCG inhibits KF proliferation. (**a**) NFs and KFs were treated with different concentrations of EGCG for the indicated time periods. The cultures were fixed, stained with a 0.01% crystal violet solution, and relative cell growth was determined as described under Materials and Methods. Data are expressed as the mean ± SE of three replicate experiments. (**b**) Serum-dependent inhibitory effects of EGCG. NFs and KFs were seeded and cultured in 10% FBS. After 6 hours, KFs were treated with different concentrations of EGCG in either high FBS (10%) or low FBS (0.2%) growth medium for 6 days. The cultures were fixed, stained with 0.01% crystal violet solution, and relative cell growth was evaluated as described under Materials and Methods. Data are expressed as the mean ± SE of three replicate of each sample. (**c**) Representative micrographs of NFs and KFs after EGCG treatment for 7 days. Bars = 200 μm. (**d**) Representative micrographs of low-cell-density seeding assay cultures after 2 weeks of EGCG treatment. (**e**) Effect of EGCG on apoptosis in KFs measured by TUNEL. KFs were treated with different concentrations of EGCG for 2 days and then labeled. TUNEL-negative cells were counted and the total number of viable cells was expressed as a percentage of control cells. Data are expressed as the mean ± SE of three replicate experiments. (**f**) KFs were seeded and cultured alone (control) or in the presence of 100 μM EGCG for 2 days. After treatment, cells were labeled with propidium iodide for 30 minutes. Labeled cells were analyzed by flow cytometry. KFs treated with 1 μM adriamycin were used as positive control for apoptosis. (**g**) Growth inhibition of KFs by EGCG is reversible. KFs were seeded and cultured in the presence or absence of 100 μM EGCG for 3 days, and then cultured for an additional 2–4 days with or without 100 μM EGCG. Relative cell growth was evaluated as above. Data are expressed as the mean ± SE of three replicate of each sample.

exclude the possibility that the growth-inhibitory mechanism of EGCG was due to an increase in cells undergoing apoptosis or replicative senescence. We also found that the decline in cell proliferation in response to EGCG treatment was reversible (Figure 1g). After incubation with 100 μM EGCG for 3 days, KFs were cultured for an additional 4 days with or without 100 μM EGCG and then analyzed as described above. In untreated controls, the total number of cells on day 7 was greater than the number of cells in the EGCG-treated plates (Figure 1g). However, growth rate of cells treated with EGCG for only the first 3 days recovered after EGCG withdrawal (relative growth per day: untreated cells, 0.391; 7-day treated cells, 0.175; 3-day treated cells, 0.236). Furthermore, it has been reported that EGCG below 100 μM can cause apoptosis of various type of cancer cells (Dreosti *et al.*, 1997; Chen *et al.*, 2003; Gupta *et al.*, 2003; Kumar *et al.*, 2007). Altogether, this result indicates that the suppressive effect of EGCG on KF proliferation was reversible. Thus, EGCG strongly suppresses the growth of KFs even though it induces a reversible cell-cycle arrest rather than a permanent exit from the cell cycle.

EGCG suppresses wound healing-related processes

Fibroblast outgrowth, collagen overproduction, and abnormal wound healing are major characteristics of keloid pathology (Al-Attar *et al.*, 2006). Proliferation and migration of fibroblasts are involved in wound healing and, therefore, expression of proliferation and migration-related proteins

may provide a useful index of therapeutic potential. In addition, c-Myc and cyclin-D1, which are key components of cell-cycle regulation, are overexpressed in, and regulate, proliferation of keloids (Chen *et al.*, 2004; Liu *et al.*, 2004). We, therefore, analyzed collagen type-I, c-Myc, and cyclin-D1 expression in KFs following EGCG treatment. Exposure to EGCG resulted in a dose-dependent decrease in collagen type-I in mRNA(α1-chain) and protein level (Figure 2a). Furthermore, we found that expression of c-Myc and cyclin-D1 was also reduced at both transcriptional and translational levels (Figure 2a).

We next determined whether EGCG inhibits migration of KFs, which is an important process in wound healing. For scratch-wound-closure assays, NFs and KFs were cultured to confluence, wounded with a 200-μl pipette tip, as described (Hu and Verkman, 2006), and treated with the indicated concentrations of EGCG (Figure 2b). Untreated KFs closed the wound within 24 hours, whereas NFs did not fully fill the wounds (wound width: NF = 83.3 ± 9.19, KF = 11.6 ± 12.02). However, EGCG strongly prevented wound closure of both NFs and KFs. Even though migratory potential of both NFs and KFs was suppressed by EGCG, their responses differed depending on the dose of EGCG. Wounds of 50 μM EGCG-treated KF cultures healed faster than those of NFs (NF: 158.1 ± 17.04, KF: 108.1 ± 7.38), but the opposite trend was observed in cultures treated with 100 μM EGCG (NF: 309.3 ± 16.71, KF: 367.7 ± 17.04). Thus, our results suggest that EGCG suppresses the migratory potential of both normal and KFs, but that this suppressive effect is greater in KFs. Taken together, these findings indicate that EGCG efficiently suppresses wound healing-related events, such as collagen production, fibroblast outgrowth, and cell migration in KFs.

EGCG regulates the PI3K, MEK/ERK, and STAT3 pathways in KFs

The above results prompted us to examine the molecular mechanisms by which EGCG suppresses proliferation and migration of KFs. Pervious researchers reported that activation of several intracellular signaling mediators, including Smad3, ERK1/2, p38 MAPK, PI3K, and STAT3, plays a role in the abnormal behavior of keloids (Tan *et al.*, 1995; Chen *et al.*, 1999; Lim *et al.*, 2003, 2006; Satish *et al.*, 2004; Kuo *et al.*, 2005; Phan *et al.*, 2005; Xia *et al.*, 2006). We, therefore, compared the phosphorylation level of these signaling pathways in normal and KFs by western blotting (Figure 3, and data not shown). Levels of phosphorylation of acutely transforming retrovirus AKT8 in rodent T-cell lymphoma (AKT), glycogen synthase kinase-3β (GSK-3β), and β-catenin did not differ between untreated normal and KFs. In contrast, phosphorylation level of Smad2/3, p38, and STAT3 (Tyr705 and Ser727) was enhanced in KFs. Interestingly, Smad2/3 was highly expressed in KFs, but Smad3 was not detectable in NFs. Decreased phosphorylation of JNK was observed in KFs. These results are consistent with the enhanced expression of collagen type-I, c-Myc, and cyclin-D1 in keloid pathology (Figure 2a), and demonstrate that phosphorylation of Smad2/3, p38, and STAT3 is augmented in KFs.

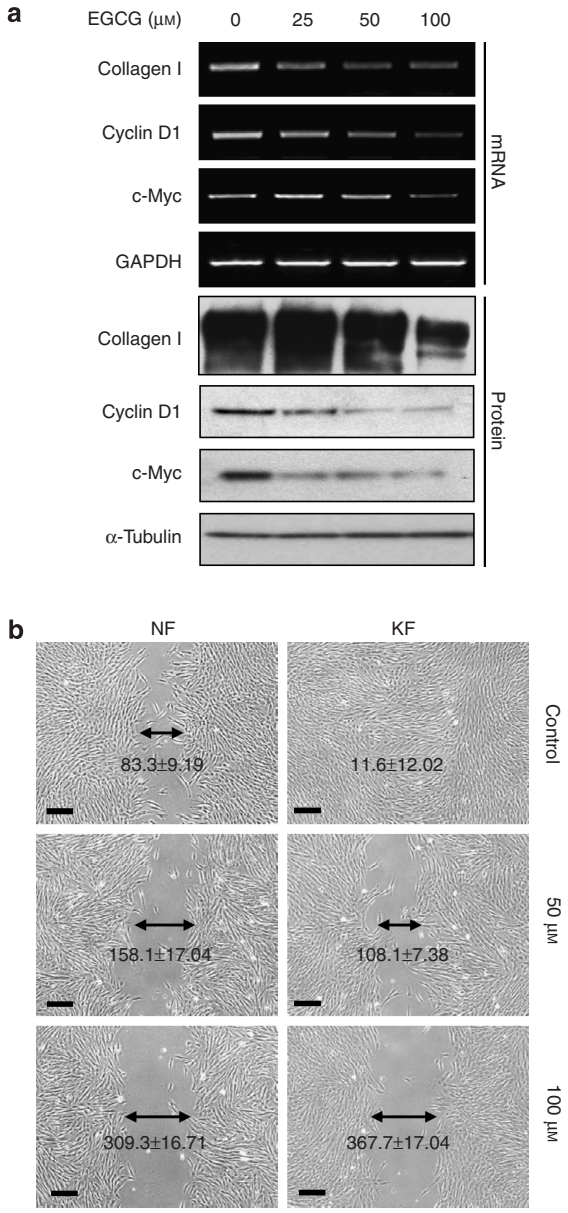

Figure 2. EGCG suppresses collagen production, cell proliferation specific marker expression, and migration in KFs. (**a**) KFs were treated with various concentrations of EGCG for 2 days. Total RNA was isolated and the expression of collagen type-I α1-chain, cyclin-D1, c-Myc, was measured by reverse transcription-PCR, with glycerladehyde-3-phosphate dehydrogenase as a loading control. Proteins, obtained from the cell lysates and cell culture supernatants (collagen type-I), were analyzed by western blot, with α-tubulin as a loading control. (**b**) Representative micrographs of scratch-wound-closure assays following EGCG treatment. NFs and KFs were synchronized for 2 hours, wounded, and treated with various concentrations of EGCG for 24 hours before being photographed. Each experiment was performed in triplicate. Arrows indicate the mean ± SE of three replicate of wound size of each sample. Bars = 200 μm.

We further analyzed which signaling mediators were regulated by EGCG in KFs. As shown in Figure 3a, phosphorylation of Smad2 and Smad3 was not affected by EGCG in KFs. Furthermore there were no remarkable changes in Smad2/3 or Smad4 expression level following EGCG

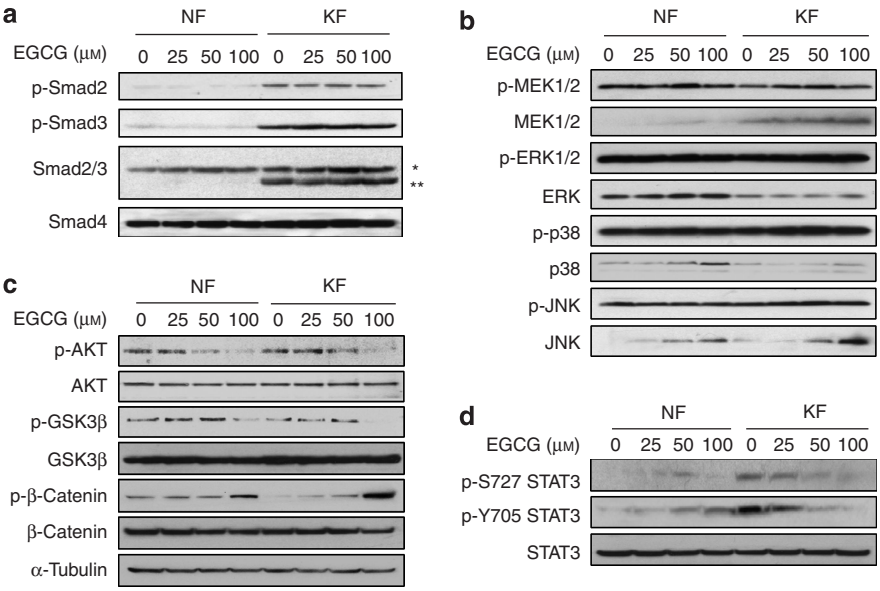

Figure 3. EGCG regulates the PI3K, MEK/ERK, and STAT3 pathways in KFs. NFs and KFs were cultured for 1.5 hours in the presence or absence of the indicated concentrations of EGCG. Total-cell lysates were prepared for western blotting. Blots were incubated with antibodies recognizing the total and phosphorylated forms of components of the (**a**) Smad pathway (*, Smad2, **, Smad3), (**b**) MAPK pathways, (**c**) PI3K/AKT pathway; and (**d**) STAT3 pathway (p-S727 STAT3, Ser727 phosphorylated STAT3; p-Y705 STAT3, Tyr705phosphorylated STAT3).

treatment. However, phosphorylated MEK/ERK level was significantly reduced within 1.5 hours of EGCG treatment (Figure 3b). EGCG treatment did not affect JNK and p38 MAPK phosphorylation, but resulted in a significant, dose-dependent reduction of phosphorylated AKT in both normal and KFs (Figure 3c). Furthermore, phosphorylation of GSK-3β and β-catenin, which are critical downstream elements of the PI3K/AKT pathway, was also regulated by EGCG in a dose-dependant manner (Figure 3c). The level of phosphorylated, inactive form of GSK-3β was significantly reduced, whereas that of the phosphorylated, degraded form of β-catenin increased, concomitant with a slight decrease in total β-catenin protein level in KFs. In addition, phosphorylation of STAT3 decreased in response to EGCG treatment. Two STAT3 residues, Tyr705 and Ser727, were highly phosphorylated in KFs, but levels of these phosphorylated forms of STAT3 were diminished by EGCG in a dose-dependant manner. Together, these results suggest that EGCG suppresses the PI3K, MEK/ERK, and STAT3 pathways, and that this suppression is correlated with proliferation and migration in KFs.

Collagen production is regulated by STAT3 signaling, not PI3K or MEK/ERK signaling, in KFs

In view of the above results, we specifically examined the roles of the PI3K, ERK, and STAT3 pathways in the expression of collagen and cell-cycle regulators using specific inhibitors for PI3K (LY294002), MEK (U0126), and JAK2/STAT3 (AG490). After synchronization in growth medium, KFs were cultured in the presence of the indicated concentrations of inhibitors for 1.5 hours or 2 days and protein extracts were then prepared for western blot analysis. As shown in Figure 4, 10 μM LY294002, 10 μM U0126, and 100 μM AG490 completely inhibited AKT, ERK1/2, and Tyr705 STAT3 phosphorylation, respectively. Higher concentrations of AG490 (200 μM) showed acute toxicity and were not used for these assays (data not shown). Treatment with 50–100 μM EGCG resulted in significant reduction of phosphorylated levels of AKT, ERK1/2, and STAT3 at Tyr705. As shown in Figure 4a, c-Myc, cyclin-D1, and collagen expression was not affected significantly by U0126 treatment. However, phosphorylation of GSK-3β was suppressed by LY294002 treatment and the total amount of β-catenin and its targets c-Myc and cyclin-D1 decreased (Figure 4b). Interestingly, neither LY294002 nor U0126 treatment affected production of collagen (Figure 4a and b). In contrast to the PI3K and MEK inhibitors, 100 μM AG490 efficiently inhibited phosphorylation of STAT3 at Tyr705, and significantly reduced collagen type-I production, similar to EGCG. In addition, expression of STAT3 targets, such as Bcl-2, cyclin-D1, c-Myc, and anti-apoptotic Bcl-xL, significantly decreased following AG490 and EGCG treatment. These data collectively show that STAT3 is the major pathway regulating collagen expression in KFs. Furthermore, neither the PI3K nor ERK1/2 pathways are required for collagen production, even though the PI3K pathway is involved in regulation of proliferation-related proteins in KFs.

STAT3 inhibition suppress proliferation and migration of KFs

We next tested whether inhibiting the PI3K, MEK/ERK, or STAT3 pathways would directly suppress proliferation and migration of KFs (Figure 5). When KFs were incubated with LY294002, their growth was inhibited in a dose- and time-dependent manner (Figure 5a, middle panel, $IC_{50} = 7.68$ μM). LY294002 at 10 μM suppressed proliferation at a rate similar to that of 100 μ EGCG. AG490 treatment also resulted in a

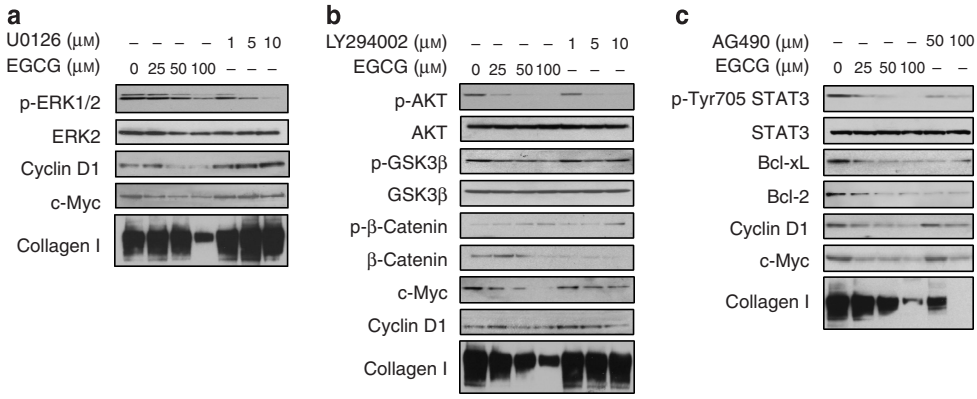

Figure 4. Effects of PI3K, ERK1/2, and STAT3 inhibitors on gene expression. KFs were cultured for 1.5 hours or 2 days (cyclin-D1, c-Myc, Bcl-2, Bcl-xL, and collagen) in the presence or absence of the indicated concentrations (μm) of (**a**) U0126; (**b**) LY294002; and (**c**) AG490. EGCG treatment is shown for comparison. Total-cell lysates and cell culture supernatants (collagen type-I) were prepared for western blotting and probed with antibodies that recognize collagen and the total and phosphorylated (p-) forms of several signaling molecules. These blots are representative of two independent experiments.

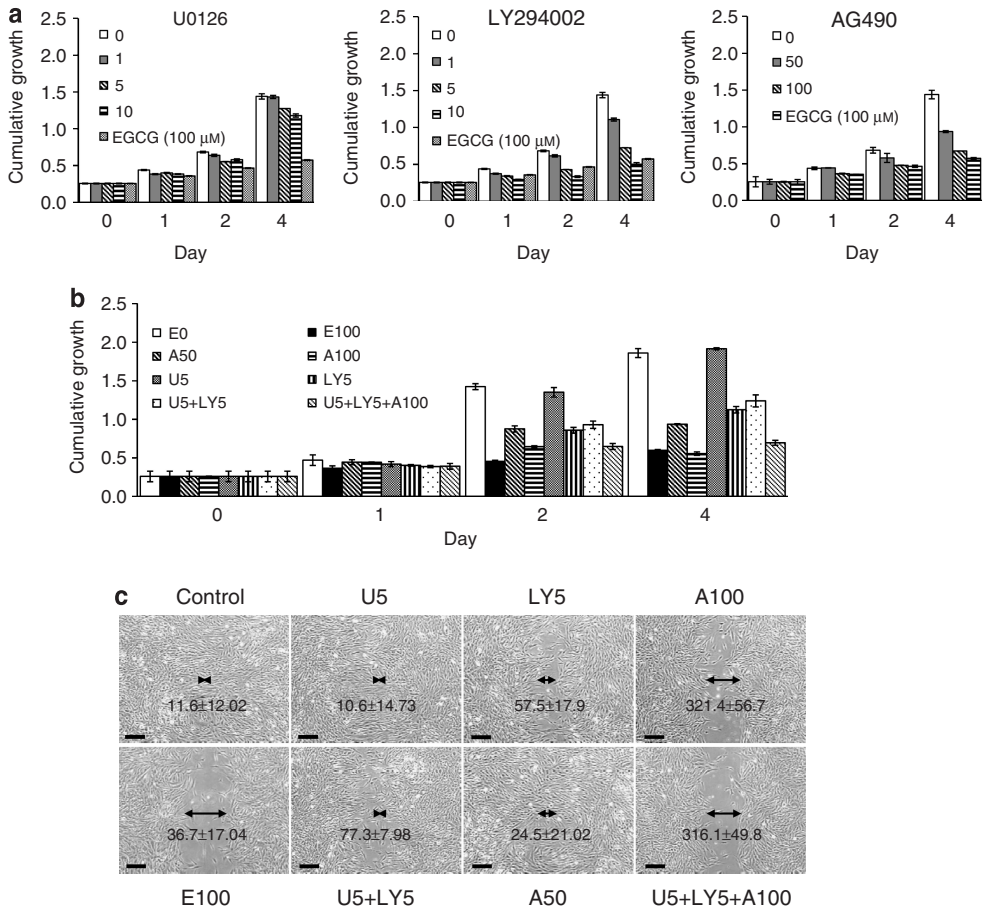

Figure 5. Effects of PI3K, ERK1/2, and STAT3 inhibitors on KF proliferation and migration. (**a**) *In vitro* proliferation assays were performed in the presence of U0126 (left panel), LY294002 (middle panel), or AG490 (right panel). KFs were seeded and treated with different concentrations (μM) of U0126, LY294002, and AG490 for the indicated times and relative cell growth was measured. Cells treated with 100 μM EGCG (E 100) were used as a positive control. Data are expressed as the mean ± SE of three replicate of each sample. (**b**) KFs were seeded and treated with 5 μM U0126 (U5), 5 μM LY294002 (L5), 50 μM AG490 (A50), and 100 μM AG490 (A100), or combinations thereof, for the indicated times and relative cell growth was measured. Cells treated with 100 μM EGCG (E100) were used as positive control. Untreated cells (E0) were used as negative control. Data are expressed as the mean ± SE of three replicate of each sample. (**c**) Confluent KFs were wounded and then treated with various combinations of inhibitors for 24 hours before being analyzed. Arrows indicate the mean ± SE of three replicates of the wound size of each sample. Bars = 200 μm.

significant reduction of proliferation of KFs (Figure 5a, right panel, $IC_{50} = 94.0\ \mu M$). However, U0126 did not suppress KF proliferation, although 10 μM U0126 completely inhibited ERK1/2 phosphorylation (Figure 5a, left panel, and Figure 4a, $IC_{50} = 27.7\ \mu M$). Together, these data indicate that the PI3K and STAT3 pathways, but not the MEK/ERK pathway, are involved in KF proliferation.

We further analyzed the effects of treatment with combinations of specific inhibitors. Because the PI3K, MEK/ERK, and STAT3 activities in KFs were all suppressed by EGCG, we predicted that combining inhibitors would recapitulate the effects observed following EGCG administration. Prior to proliferation assays, we determined the concentrations of LY294002, U0126, and AG490 required for inhibiting phosphorylation of AKT, ERK, and STAT3 at Tyr705 to extents similar to that with 100 μM EGCG treatment. As shown in Figure 4, treatment with 5 μM LY294002, 5 μM U0126, or 100 μM AG490 blocked AKT, ERK1/2, and Tyr705 STAT3 phosphorylation, respectively, to the same extent as with 100 μM EGCG. We then cultured KFs with U0126 (5 μM), LY294002 (5 μM), and AG490 (50–100 μM), alone or in combination. LY294003 inhibited the growth of KFs, but not to the extent as that with 100 μM EGCG treatment. In contrast, U0126 had no effect on cell growth (Figure 5b). However, AG490 strongly suppressed the growth of KFs as much as 100 μM EGCG did. Furthermore, combined treatment with AG490, LY294002, and U0126 did not further suppress proliferation compared with treatment with AG490 alone (Figure 5b).

Similar patterns were observed in the wound-closure assay (Figure 5c). Neither LY294002 nor the LY294002/U0126 combination significantly suppressed migration. However, incubation with AG490, alone or in combination with the other inhibitors, strongly suppressed migration of KFs. These findings suggest that EGCG blocks keloid pathology by suppressing STAT3 and that the PI3K- and MEK/ERK-signaling pathways, although inhibited by EGCG, do not play a critical role in keloid pathology.

Proliferation and migration of KFs is inhibited by STAT3 siRNAs and cucurbitacin-I

To confirm the role of STAT3 in migration of KFs, fibroblasts were transfected with siRNAs targeting STAT3 and wound-closure assays were performed. Before wound-closure assays, we verified STAT3 inhibition by western blotting. As shown in Figure 6a, STAT3 siRNA-1 had the strongest suppressive effect on STAT3 expression, although all STAT3 siRNAs inhibited STAT3 expression to some degree. Interestingly, siRNA suppression of STAT3 was highly correlated with reduced expression of collagen type-I, c-Myc, and cyclin-D1. Consistent with the western blotting results, STAT3 siRNA-1 significantly suppressed KF migration into scratch wounds,

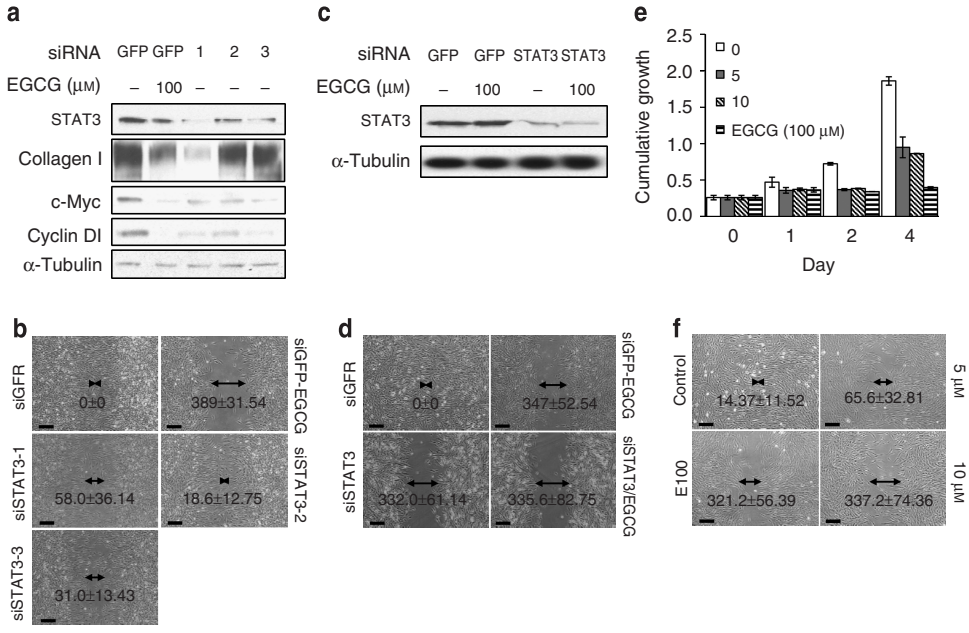

Figure 6. Effects of STAT3 siRNAs and cucurbitacin-I on proliferation and migration of KFs. (**a**) KFs were transfected with STAT3 siRNAs (siRNAs 1–3) and GFP siRNA (negative control) and subsequently cultured 72 hours. Total-cell lysates and cell culture supernatants (collagen type-I) were prepared for western blotting and probed with antibodies recognizing STAT3, collagen type-I, c-Myc, cyclin-D1, and α-tubulin. (**b**) *In vitro* scratch-wound-closure assays with STAT3 siRNA- and GFP siRNA-transfected KFs. STAT3 siRNA- and GFP siRNA-transfected KFs were collected 48 hours after transfection and replated at confluent densities. KFs were synchronized for 2 hours, wounded, and cultured in the presence or absence of EGCG for 24 hours before being photographed. Each experiment was performed in triplicate. Arrows indicate the average size of wounds. Bars = 200 μm. (**c**) KFs were co-transfected with STAT3 siRNAs-co-transfected and GFP siRNA-transfected and subsequently cultured 72 hours. Total-cell lysates were prepared for western blotting and probed with antibodies recognizing STAT3 and α-tubulin. (**d**) *In vitro* scratch-wound-closure assays with STAT3 siRNA-co-transfected and and GFP siRNA-transfected KFs. Arrows indicate the average size of wounds. Bars = 200 μm. (**e**) *In vitro* proliferation assays were performed in the presence of cucurbitacin-I and EGCG. (**f**) *In vitro* scratch-wound-closure assays in KFs treated with cucurbitacin-I or EGCG. Bars = 200 μm.

but green fluorescent (GFP) siRNA-transfected KFs healed the wounds (Figure 6b). We further evaluate the effect of EGCG in fibroblasts pretreated with the siRNA STAT3. For complete inhibition of STAT3, we co-transfected all STAT3 siRNAs and performed wound-closure assays. Co-transfection of siRNA STAT3s almost completely blocks STAT3 protein expression and strongly suppressed KF migration into scratch wounds (Figure 6c and d). Upon EGCG treatment of siRNA-transfected KFs, cell migration of STAT3 siRNA-co-transfected KFs was not decreased significantly(Figure 6d). This result implied that STAT3 inhibition might be the major mechanism for suppression of KF migration by EGCG.

We also examined proliferation and migration of KFs treated with cucurbitacin-I, known as another inhibitor specific to JAK/STAT3 but not Ras, ERK1/2, or JNK pathways (Blaskovich *et al.*, 2003). Proliferation assays were performed on cultures treated with 5 or 10 μM cucurbitacin-I. As shown in Figure 6e, cucurbitacin-I treatments decreased proliferation of KFs, but not to the extent as observed with 100 μM EGCG treatment. In contrast, 10 μM cucurbitacin-I suppressed cell migration more strongly than EGCG (Figure 6f). Together, these data demonstrate that STAT3 is an important signal mediator of proliferation and migration in KFs.

EGCG suppresses nodule development and collagen production in an *in vivo* keloid model

To evaluate the therapeutic potential of EGCG in treatment of keloids, we implanted normal and KFs into the backs of nude mice and they were randomly grouped 7 days after implantation and treated by intra-lesional injection with 1.25 mg per nodule EGCG or phosphate-buffered saline (PBS). At day 17, the size of KFs nodules was twice that of NF nodules (Figure 7b). However, EGCG treatment markedly reduced nodule size compared with that in untreated keloid nodules. The average weight of keloid nodules was decreased by EGCG treatment, and was similar to that of NF nodules (Figure 7b). The average inhibition ratio of EGCG was 58%. Histologically, cellularity of KF nodules were higher than that of NF nodules (Figure 7c, upper panel). In addition, blood vessels were well developed around the keloid nodules, but not around NF nodules (Figure 7a). However, EGCG treatment suppressed cellularity and blood vessel formation around the keloid nodules. There was no significant change in the weight and appearance of mice in any of the experimental groups. We examined collagen production by immunohistochemistry. As illustrated in Figure 7c, collagen fibers were prominent in the nodules of KFs, but not in those of NFs. However, collagen accumulation of keloid nodules was repressed by EGCG treatment. Moreover, STAT3 phosphorylation at Tyr705 was also suppressed in EGCG-treated keloid nodules (Figure 7c). These observations suggest that EGCG inhibits keloid development and collagen production by STAT3 suppression in an *in vivo* model.

DISCUSSION

Keloids are benign cutaneous tumors that develop after dermal injury and exhibit vigorous and continuous production of collagen (Rekha, 2004). Many groups have explored the potential relationship between the abnormal expression of growth factors and cytokines and cell migration (Phan *et al.*, 2004, 2005; Sato, 2006). TGF-β, platelet-derived growth factor, epidermal growth factor, VEGF, connective tissue growth factor, and IL-6 have all been reported to play an important role in keloid pathology (Tan *et al.*, 1995; Satish *et al.*, 2004; Khoo *et al.*, 2006; Wu *et al.*, 2006). These factors accelerate migration by stimulating collagen production and proliferation of KFs *in vitro*. Most growth factors and cytokines transmit their signals through cognate receptors linked to specific intracellular signaling pathways. Interestingly, however, in keloid development, common intracellular pathways are stimulated by a number of different growth factors.

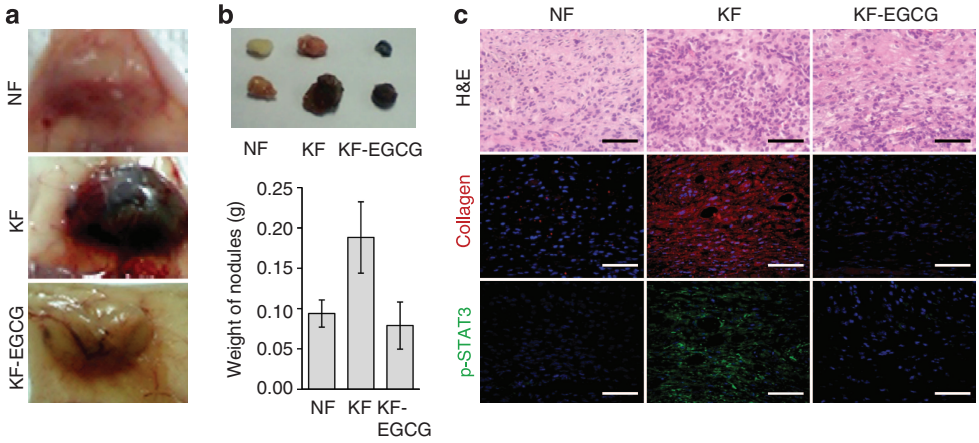

Figure 7. EGCG suppresses growth and collagen production in an *in vivo* keloid model. (**a**) Representative photographs of NF and KF nodules embedded in the panniculus muscle of nude mice. Mice were randomly grouped 7 days after implantation and treated by intra-lesional injection with 1.25 mg per nodule EGCG or vehicle (PBS). All animals were killed 17 days after implantation and keloid nodules were excised (NF, NF-derived nodules; KF, KF-derived nodules; KF-EGCG, EGCG-treated nodules derived from KFs). (**b**) Representative photographs of NF and KF nodules excised from the panniculus muscle of nude mice (upper panel) and average weight of excised nodules (lower panel). (**c**) Hematoxylin and eosin (H&E, upper panel), anti-human collagen (middle panel), and p-Tyr705 STAT3 (lower panel) antibody staining of normal and KF nodules. Bars = 50 μm.

EGCG, the most abundant polyphenol in green tea, shows various pharmacological effects, including antitumor activity, by regulating multiple signaling pathways, with a wide range of health benefits. In skin tumors, topical treatment or oral consumption of green tea polyphenols or EGCG inhibits chemical carcinogen- or UV radiation-induced skin carcinogenesis in different animal models (Luo *et al.*, 2001; Al-Attar *et al.*, 2006). Furthermore, the apoptotic effects of EGCG are highly selective for tumor cells, leaving normal tissues undamaged (Ahn *et al.*, 1999; Wang and Bachrach, 2002; Paul *et al.*, 2005). In addition, the safety of EGCG has been demonstrated by many research groups (Kubota *et al.*, 2002; Ullmann *et al.*, 2003; Kumar *et al.*, 2007). Thus, EGCG has been studied extensively as a potential treatment for various types of tumors.

Here, we further explored the pharmacological potential of EGCG in treatment of keloids using *in vitro* and *in vivo* KF models. These models are useful as the abnormalities observed in keloids, such as hyperproliferation and collagen overproduction, are mostly mediated by KFs and can be recapitulated. We demonstrated here that EGCG suppresses proliferation and migration of NFs and KFs (Figures 1 and 2). However, EGCG had a stronger effect on KFs, since EGCG's IC_{50} for proliferation was higher in NFs (NF: 63.0 μM *versus* KF: 54.4 μM, on day 7). In addition, EGCG inhibits KF proliferation by cell-cycle arrest rather than inducing a permanent exit from the cell cycle. These data imply that EGCG suppresses keloid development without damaging normal skin. These findings are consistent with a previous report that EGCG suppresses adhesion-related signaling in NFs, without cytotoxic or proapoptotic activity (Hung *et al.*, 2005).

Our results have also demonstrated that phosphorylation of Smad2/3, p38, and STAT3 is greatly enhanced in KFs, but phosphorylation of the AKT pathway components is similar to that in NFs. These data imply that Smad2/3, p38, and STAT3 may be suitable therapeutic targets for keloids, as the phosphorylation level of these signaling pathways differs from that in normal tissue. EGCG inhibits one of these KF-activated pathways, the STAT3 pathway.

The relationship between keloids and STAT3 activity was recently demonstrated (Lim *et al.*, 2006) by showing that STAT3 contributes to keloid pathogenesis by promoting collagen production, cell proliferation, and migration. This report is consistent with our findings presented here. We found that EGCG blocked STAT3 phosphorylation (Tyr705 and Ser727) and that inhibition of STAT3 by AG490, STAT3 siRNA, and cucurbitacin-I decreased collagen production, proliferation, and migration of KFs. STAT3 is an oncogene and a latent transcription factor that is involved in diverse processes, including cell proliferation, migration, inflammation, immune responses, and cell survival. It is activated by various growth factors and cytokines, including platelet-derived growth factor, VEGF and IL-6, which have also been linked to keloid pathology (Darnell, 1997). These reports and our findings presented here suggest that EGCG suppresses keloid development. EGCG is likely to regulate signaling mediated by a number of soluble factors, since no single unifying factor that is responsible for keloid formation has been identified.

EGCG suppresses the PI3K, MEK/ERK, and STAT3 pathways in KFs. However, treatment with combinations of inhibitors demonstrated that PI3K and MEK/ERK signaling did not contribute to proliferation and migration, but the STAT3-signaling pathway did (Figure 5b and c). Furthermore, EGCG did not synergically suppress migration of STAT3 siRNA-co-transfected KFs even though PI3K- and MEK/ERK-signaling pathways were strongly suppressed by EGCG (Figure 6d). This result is inconsistent with previous reports (Mirza *et al.*, 2000; Lorenzini *et al.*, 2002; Lim *et al.*, 2003), which demonstrated that the PI3K and ERK1/2 pathways do play a role in cell proliferation, survival, and collagen expression in KFs. These differences may be the result of differences in the signaling status of KFs due to different cell culture systems and patient variations. For example, we cultured normal and KFs in low-glucose DMEM medium with 10% fetal bovine serum (FBS), because high glucose (hyperglycemic medium) induces premature replicative senescence in NFs (Blazer *et al.*, 2002). In the low-glucose culture medium, we cultured two patient-derived KFs for more than 30 passages, which is three times longer than their previously reported lifespan in culture (Yamamoto and Inoue, 1982).

Dexamethasone, which is the most common keloid therapeutic agent, induces keloid regression through suppression of VEGF expression and KF proliferation (Wu *et al.*, 2006). Because EGCG inhibits VEGF expression in human breast cancer cells (Masuda *et al.*, 2002), we hypothesized that EGCG and dexamethasone may suppress keloid's pathology through similar mechanisms. We observed proliferation and migration of KFs following EGCG and dexamethasone treatment (Figure S2). In our experimental system, the KF proliferation rate after 7 days of dexamethasone treatment was reduced, but not to the extent as observed after EGCG treatments of the same length. Furthermore, dexamethasone did not significantly inhibit migration or alter the morphology of KFs. We also investigated the effect of EGCG and dexamethasone treatment on VEGF expression in KFs (Figure S2c). Both EGCG and dexamethasone inhibited VEGF expression at the mRNA level. Furthermore, we observed that EGCG treatment suppressed blood vessel formation around keloid nodules (Figure 7b). Taken together, these results imply that EGCG could be a more effective therapeutic agent for keloids than dexamethasone, even though the two chemicals share a common target molecule, VEGF.

To use EGCG as a therapeutic agent, optimal concentrations and treatment methods should be determined. We used a range of EGCG concentrations, from 25 to 100 μM, in the *in vitro* studies and 1.25 mg per nodule in the *in vivo* study. In contrast, pharmacokinetic studies conducted on humans indicate that the physiologically relevant serum concentrations of EGCG may be in the high nanomolar range by daily oral administration. Therefore, topical or intra-lesional administration of EGCG may be a more effective option for keloid therapy. A clinical study examining the ability of either topical or oral administration of green tea extract products to

reduce the appearance of photoaging skin (Chiu *et al.*, 2005) demonstrated that topical administration of EGCG more effectively protected against UV-induced damage to the skin. Furthermore, we observed that intra-lesional injections of 1.25 mg per nodule ($\approx$62 mg kg^{-1}) EGCG inhibited keloid development without systemic health damage. In addition, it had been reported that a dose of 200 mg EGCG per kg induced no toxicity (Kubota *et al.*, 2002; Ullmann *et al.*, 2003; Isbrucker *et al.*, 2006; Kumar *et al.*, 2007).

In summary, we have demonstrated that EGCG suppresses the pathological characteristics of KFs by inhibiting STAT3 signaling. Although EGCG inhibits PI3K and MEK/ERK signaling, modulation of these pathways did not further block proliferation, migration, or collagen production in KFs treated with STAT3 inhibitors. Together, these results suggest that EGCG could be used as a safe, alternative keloid therapeutic agent.

MATERIALS AND METHODS

Reagents

U0126 was purchased from Promega (Madison, WI). LY294002, EGCG, and a mouse anti-α-tubulin antibody were purchased from Sigma-Aldrich (St Louis, MO). Rabbit anti-cyclin-D1 and rabbit anti-c-Myc antibodies were obtained from Santa Cruz Biotechnology (Santa Cruz, CA). Rabbit anti-phospho-Thr180/Tyr182 p38 antibodies were purchased from Abcam (Cambridge, UK). Rabbit anti-phospho-MAPK 1/2 (ERK1/2), anti-phospho-Thr183/Tyr185-JNK, and anti-phospho-Thr221/Thr223-JNK antibodies were purchased from Upstate (Chicago, IL). Anti-AKT, anti-phospho-Ser473-AKT, anti-GSK-3β, anti-phospho-Ser9-GSK-3β, anti-β-catenin, anti-phospho-Ser33/37/Thr41-β-catenin, anti-phospho-Ser217/221-MEK 1/2, anti-STAT3, anti-phospho-Tyr705-STAT3, anti-phospho-Ser727-STAT3, anti-Smad2/3, anti-phospho-Smad2, anti-phospho-Smad3, anti-Smad4, and anti-Bcl-xL antibodies were all rabbit polyclonal antibodies and were obtained from Cell Signaling (Danvers, MA). The mouse anti-collagen type-I antibody was purchased from R&D Systems (Minneapolis, MN). Horseradish peroxidase-conjugated goat anti-mouse and anti-rabbit secondary antibodies were purchased from Zymed (South San Francisco, CA). The chemiluminescence detection system was from Pierce (Rockford, IL). Tissue culture dishes, six-well plates, and 96-well plates were purchased from Nunc (Naperville, IL).

U0126, LY294002, AG490, and cucurbitacin-I are MEK1/2-, PI3K-, and JAK2/STAT3-specific inhibitors, respectively. They were dissolved in DMSO (with final concentration not exceeding 0.1%) and stored in a frozen condition, at −20 °C, away from light. The final concentration of DMSO in experimental treatments never exceeded 0.1%. Stock solutions of EGCG in DMEM (Hyclone, Logan, UT) without FBS were stored at −70 °C.

Normal and KF culture

Primary normal and KF cultures were established as described previously (Blazer *et al.*, 2002; Lim *et al.*, 2006). Normal (three patients) and keloid (two patients) tissues obtained from patients undergoing surgical excision were collected aseptically in a tube containing low-glucose (1000 mg ml^{-1}) DMEM and antibiotics (penicillin 100 U ml^{-1}, streptomycin 100 μg ml^{-1}) (Gibco, Grand Island, NY). Samples of dermis were washed twice with a PBS containing antibiotics and were incubated in a solution of collagenase type-I (0.5 mg ml^{-1}) and trypsin (0.2 mg ml^{-1}) for 6 hours at 37 °C. Cells were pelleted and then cultured in tissue culture flasks. Isolated fibroblasts were cultured in low-glucose DMEM supplemented with 10% FBS, 2 mM L-glutamine, and antibiotics. After reaching confluence, cells were treated with 0.05% trypsin (Gibco) and collected for subculturing. Cultured fibroblasts that had been passaged less than eight times were used for all the experiments. All studies strictly adhered to the guidelines of the Institutional Review Board of Korea University. This study was conducted according to the Declaration of Helsinki Principles.

In vitro scratch-wound-closure assays

In vitro scratch-wound-closure assays were performed as previously described (Hu and Verkman, 2006). Cells were seeded into six-well dishes at a density of 7×10^5 cells per well. The dishes were cultured as confluent monolayers, synchronized in low-glucose DMEM containing 10% FBS for 2 hours, and wounded by removing a 300–500 μm-wide strip of cells across the well with a standard 200 μl pipette tip. The wounded culture wells were washed twice with PBS to remove non-adherent cells, and treated with various inhibitors. Wound-closure effects were observed at least 24 hours later.

In vitro proliferation and low-density seeding assay

Cell growth was determined by plating cells at a density of 2×10^4 (proliferation assay) or 10^2 cells per well (low density seeding assay) in six-well plates and synchronizing them in low-glucose DMEM containing 10% FBS. The inhibitors U0126, LY294002, AG490, cucurbitacin-I, and EGCG were added to triplicate wells 6 hours after plating and cells were cultured for the indicated times. For the low-density seeding assay, cells were cultured more than 2 weeks. Cells were then fixed with 10% formalin and stained with 0.01% crystal violet. Crystal violet from stained cells was extracted using 10% acetic acid and quantified spectrophotometrically (600 nm) to determine relative cell growth rates.

Senescence-associated β-galactosidase staining

Cell senescence was measured by senescence-associated β-galactosidase staining (You *et al.*, 2004). Briefly, cells were grown in 60-mm cell culture dishes, washed three times with PBS, and fixed with 2% formaldehyde/0.2% glutaraldehyde in PBS for 10 minutes. The cells were then washed and incubated with β-galactosidase substrate solution (150 mM NaCl, 2 mM $MgCl_2$, 5 mM potassium ferricyanide, 5 mM potassium ferrocyanide, 40 mM citric acid, and 12 mM sodium phosphate, pH 6, containing 1 mg ml^{-1} 5-bromo-4-chloro-3-indolyl-β-*d*-galactoside (X-gal)) for 24 hours at 37 °C.

Cell-cycle analysis by flow cytometry

For cell-cycle analysis, flow cytometry was performed as previously described (Sah *et al.*, 2004). Cells were seeded into 100-mm dishes at a density of 7×10^5 cells per dish, allowed to attach overnight, and then treated with various concentrations of EGCG in culture medium for 48 hours. Cells were harvested with trypsin and washed twice before fixing with methanol overnight. The cells were incubated in propidium iodide for an additional 30 minutes. The labeled cells were analyzed by flow cytometry. Apoptosis was quantified by measuring the sub-G_1/S DNA content.

TUNEL assay

Apoptotic cells were detected using the TACS-XL *In situ* Apoptosis Detection kit according to the manufacturer's instructions (R&D System). Briefly, KFs were seeded in six-well plates at a density of 10^4 cells per well and then incubated with varying doses of EGCG. After the indicated times, cells were fixed and treated with proteinase-K for permeabilization. The apoptotic DNA fragments were labeled with biotinylated nucleotides using terminal deoxynucleotidyl transferase. The biotinylated nucleotides were then detected using a streptavidin–horseradish peroxidase conjugate and diaminobenzidine. The numbers of TUNEL-positive cells were counted, and at least 10,000 cells in five randomly selected microscopic fields were scored for each group ($n=3$).

Semi-quantitative reverse transcription-PCR

Total RNA was prepared using Trizol reagent (Invitrogen, Carlsbad, CA). Standard reverse transcription was performed using 500 ng of total RNA, an oligo-d$(T)_{12-18}$ primer (Gibco), and superscriptase II (Invitrogen). Reverse transcription-PCR used 1 μl of cDNA template, 10 pmol of primers, and a PCR premix (1 U *Taq* DNA polymerase, 250 μM dNTPs, 10 mM Tris-HCl, 40 mM KCl and 1.5 mM $MgCl_2$; Bioneer, Seoul, Korea). PCR analysis was performed using the following primers: c-Myc, 5′-TCGGATTCTCTGCTCTCCTC-3′, 5′-CGCCTCTTGACATTCTCCTC-3′; cyclin-D, 5′-CAAATGTGTGCAGAAGGAGG-3′, 5′-CTGGCATTTTGGAGAGGAAG-3′; collagen type-I α1-chain, 5′-CACAGAGGTTTCAGTGGTTTGG-3′, 5′-GCACCAGTAGCACCATCATTTC-3′; VEGF, 5-GAAACCATGAACTTTCTGCTG-3, 5-TCCTTCCTCTGCCCGGCTA-3; glycerladehyde-3-phosphate dehydrogenase, 5′-GTGGTCTCCTCTGACTTCAACA-3′, 5′-CTCTTCCTCTTGTGCTCTTGCT-3′. All primer pairs had a calculated annealing temperature of 62 °C. PCR was conducted using GeneAmp 9600 (Perkin Elmer, Boston, MA) with a 5-minute denaturation step at 94 °C, 30 cycles of 94 °C for 30 seconds, 62 °C for 30 seconds, and 72 °C for 30 seconds, and a final extension for 10 minutes at 72 °C. PCR amplifications were verified to be in the linear range.

Western blot analysis

To detect protein expression and modification in response to treatment with U0126, LY294002, AG490 and EGCG, cells plated at a density of 5×10^5 cells per dish were cultured for the indicated times (1.5 hours or 2 days) in growth medium in the presence or absence of inhibitors. Total protein was extracted with radioimmunoprecipitation assay buffer (50 mM Tris-HCl pH 7.5, 150 mM NaCl, 1% Nonidet-40 (NP-40), 0.5% sodium deoxycholate, 1% SDS, 1 mM sodium orthovanadate, 1 mM β-glycerol phosphate, 1 mM sodium fluoride, 2.5 mM sodium pyrophosphate) containing a protease inhibitor cocktail (Roche, Nutley, NJ). Lysates were centrifuged at 12,000 *g* for 30 minutes at 4 °C. Protein concentrations were determined using the Bradford assay kit (BioRad, Hercules, CA). Protein (50 μg) was separated using precast 4–12% gradient SDS-PAGE (Invitrogen) and transferred onto polyvinylidene difluoride membranes (Invitrogen). Blots were incubated with the indicated primary antibodies and horseradish peroxidase-conjugated goat anti-mouse or anti-rabbit secondary antibodies (1:2,000 dilution). All of the primary antibodies were used at a final concentration of 1 μg ml^{-1}. Blots were then visualized using a chemiluminescence detection system as recommended by the manufacturer (Pierce).

For detecting collagen expression in cell culture supernatants, 2-day-cultured conditioned media were collected, concentrated 10 times with Centricon Centrifugal Filter (30-kDa cut-off) and blotted described above.

siRNA transfection

Cells were treated with an siRNA for either 48 or 72 hours. Cells were transfected with siRNA overnight with Oligofectamine (Invitrogen) in Opti-MEM (Invitrogen) and supplemented with 10% FBS the next morning. The concentration of siRNA was 3 μmol per 100-mm dish. For complete inhibition of STAT3, all STAT3 siRNAs (STAT3 siRNAs 1–3) were co-transfected at the concentration of 2 μmol per 100-mm dish of each STAT3 siRNAs. STAT3 siRNAs 1–3 were purchased from Bioneer. Cells were assayed by western blotting and *in vitro* wound-closure assay 48 hours after transfection.

Implantation of cultured human fibroblasts into nude mice and EGCG treatment

We tested the therapeutic potential of EGCG in treatment of keloids using an *in vivo* model (Fujiwara *et al.*, 2005; Zhu *et al.*, 2007). Briefly, keloid and NFs were implanted into the dorsal area of BALB/c nude mice weighing 18–22 g (Central Lab. Animal Inc., Seoul, Korea). Fibroblasts (5×10^8 cells per injection) were injected into the panniculus muscle using a syringe with a 26-gauge needle (Korea Vaccine Co. Ltd, Seoul, Korea). At 7 days post implantation, mice were randomly grouped and given intra-lesion injections of 1.5 mg per nodule of EGCG or the vehicle (PBS). At 17 days post implantation, all animals were killed and keloid nodules were excised and weighed. The nodule growth ratio was calculated as follows:

$$\text{Inhibition ratio}\,(\%) = [(C-T)/C]\times100\%$$

where C represents the average nodule weight of the control group and T is the average nodule weight of EGCG-treated mice. Some nodule tissues were fixed in formaldehyde for immunohistochemical analysis. All studies were conducted in strict adherence to the guidelines of the Institutional Review Board of Korea University.

Hematoxylin and eosin staining

Normal and keloid nodules were fixed with 4% paraformaldehyde in PBS, embedded in paraffin, and sectioned. Tissue sections were stained with hematoxylin for 5–8 minutes, washed with running water, quickly destained with acid ethanol containing 1% hydrochloric acid and 70% ethanol, washed with running water, and counterstained with eosin–ethanol for 3–5 minutes. Tissue sections were then rehydrated by gradual immersion in 70, 80, 95, and 100% ethanol, cleared with xylene, and finally mounted in entellan.

Immunohistochemistry

Normal and keloid nodules after formaldehyde fixation and paraffin embedding was cut into three fragments with 5 ~ 6 μm thickness. It is then washed with xylene to remove paraffin and immunohistochemical staining was performed on each fragment for human collagen, and p-Tyr705 STAT3. To maintain antigenicity of protein, the microwave oven method was used to treat it in boiling PBS, and hydrogen peroxide was applied to inhibit any activation of intrinsic peroxidase. After that, primary antibodies against human collagen and p-Tyr705 STAT3, which were diluted at a 1:100 ratio, were

induced to show reactions at room temperature for 2 hours. The secondary FITC or Cy3-labeled antibodies (LSAB kit; Dako, Glastrup, Denmark) was induced to show reaction for 20 minutes and then washed in PBS. Sections were washed again and mounted with Vectashield mounting medium containing 4,6-diamidino-2-phenylindole (DAPI). Picture was taken with Olympus DP 70 Digital Camera System. (Olympus, Tokyo, Japan).

CONFLICT OF INTEREST

The authors state no conflict of interest.

ACKNOWLEDGMENTS

This work was supported by a BioGreen 21 grant to Seungkwon You.

SUPPLEMENTARY MATERIAL

Figure S1. EGCG does not induce apoptosis.

Figure S2. EGCG has a stronger inhibitory effect on KF proliferation and migration than dexamethasone.

REFERENCES

Ahn HY, Hadizadeh KR, Seul C, Yun YP, Vetter H, Sachinidis A (1999) Epigallocathechin-3 gallate selectively inhibits the PDGF-BB-induced intracellular signaling transduction pathway in vascular smooth muscle cells and inhibits transformation of sis-transfected NIH 3T3 fibroblasts and human glioblastoma cells (A172). *Mol Biol Cell* 10: 1093–104

Al-Attar A, Mess S, Thomassen JM, Kauffman CL, Davison SP (2006) Keloid pathogenesis and treatment. *Plast Reconstr Surg* 117:286–300

Blaskovich MA, Sun J, Cantor A, Turkson J, Jove R, Sebti SM (2003) Discovery of JSI-124 (cucurbitacin I), a selective Janus kinase/signal transducer and activator of transcription 3 signaling pathway inhibitor with potent antitumor activity against human and murine cancer cells in mice. *Cancer Res* 63:1270–9

Blazer S, Khankin E, Segev Y, Ofir R, Yalon-Hacohen M, Kra-Oz Z *et al.* (2002) High glucose-induced replicative senescence: point of no return and effect of telomerase. *Biochem Biophys Res Commun* 296: 93–101

Chen C, Shen G, Hebbar V, Hu R, Owuor ED, Kong AN (2003) Epigallocatechin-3-gallate-induced stress signals in HT-29 human colon adenocarcinoma cells. *Carcinogenesis* 24:1369–78

Chen SJ, Yuan W, Mori Y, Levenson A, Trojanowska M, Varga J (1999) Stimulation of type I collagen transcription in human skin fibroblasts by TGF-beta: involvement of Smad 3. *J Invest Dermatol* 112:49–57

Chen W, Fu XB, Ge SL, Sun XQ, Zhou G, Zhao ZL *et al.* (2004) Development of gene microarray in screening differently expressed genes in keloid and normal-control skin. *Chin Med J (England)* 117:877–81

Chiu AE, Chan JL, Kern DG, Kohler S, Rehmus WE, Kimball AB (2005) Double-blinded, placebo-controlled trial of green tea extracts in the clinical and histologic appearance of photoaging skin. *Dermatol Surg* 31:855–60, discussion 860

Darnell JE Jr (1997) STATs and gene regulation. *Science* 277:1630–5

DiPaola RS (2002) To arrest or not to G(2)-M cell-cycle arrest: commentary re: AK Tyagi *et al.*, Silibinin strongly synergizes human prostate carcinoma DU145 cells to doxorubicin-induced growth inhibition, G(2)-M arrest, and apoptosis. *Clin Cancer Res*, 8: 3512–3519, 2002. *Clin Cancer Res* 8:3311–4

Dreosti IE, Wargovich MJ, Yang CS (1997) Inhibition of carcinogenesis by tea: the evidence from experimental studies. *Crit Rev Food Sci Nutr* 37:761–70

Ehrlich HP, Desmouliere A, Diegelmann RF, Cohen IK, Compton CC, Garner WL *et al.* (1994) Morphological and immunochemical differences between keloid and hypertrophic scar. *Am J Pathol* 145:105–13

Fujiwara M, Muragaki Y, Ooshima A (2005) Upregulation of transforming growth factor-beta1 and vascular endothelial growth factor in cultured keloid fibroblasts: relevance to angiogenic activity. *Arch Dermatol Res* 297:161–9

Gupta S, Hussain T, Mukhtar H (2003) Molecular pathway for (−)-epigallocatechin-3-gallate-induced cell cycle arrest and apoptosis of human prostate carcinoma cells. *Arch Biochem Biophys* 410:177–85

Hu J, Verkman AS (2006) Increased migration and metastatic potential of tumor cells expressing aquaporin water channels. *FASEB J* 20:1892–4

Hung CF, Huang TF, Chiang HS, Wu WB (2005) (−)-Epigallocatechin-3-gallate, a polyphenolic compound from green tea, inhibits fibroblast adhesion and migration through multiple mechanisms. *J Cell Biochem* 96:183–97

Isbrucker RA, Edwards JA, Wolz E, Davidovich A, Bausch J (2006) Safety studies on epigallocatechin gallate (EGCG) preparations. Part 2: dermal, acute and short-term toxicity studies. *Food Chem Toxicol* 44:636–50

Kada T, Kaneko K, Matsuzaki S, Matsuzaki T, Hara Y (1985) Detection and chemical identification of natural bio-antimutagens. A case of the green tea factor. *Mutat Res* 150:127–32

Kelly AP (2004) Medical and surgical therapies for keloids. *Dermatol Ther* 17:212–8

Khoo YT, Ong CT, Mukhopadhyay A, Han HC, Do DV, Lim IJ *et al.* (2006) Upregulation of secretory connective tissue growth factor (CTGF) in keratinocyte-fibroblast coculture contributes to keloid pathogenesis. *J Cell Physiol* 208:336–43

Kubota Y, Umegaki K, Tanaka N, Mizuno H, Nakamura K, Kunitomo M *et al.* (2002) Safety of dietary supplements: chronotropic and inotropic effects on isolated rat atria. *Biol Pharm Bull* 25:197–200

Kumar N, Shibata D, Helm J, Coppola D, Malafa M (2007) Green tea polyphenols in the prevention of colon cancer. *Front Biosci* 12:2309–15

Kuo YR, Wu WS, Jeng SF, Huang HC, Yang KD, Sacks JM *et al.* (2005) Activation of ERK and p38 kinase mediated keloid fibroblast apoptosis after flashlamp pulsed-dye laser treatment. *Lasers Surg Med* 36:31–7

Lim CP, Phan TT, Lim IJ, Cao X (2006) Stat3 contributes to keloid pathogenesis via promoting collagen production, cell proliferation and migration. *Oncogene* 25:5416–25

Lim IJ, Phan TT, Tan EK, Nguyen TT, Tran E, Longaker MT *et al.* (2003) Synchronous activation of ERK and phosphatidylinositol 3-kinase pathways is required for collagen and extracellular matrix production in keloids. *J Biol Chem* 278:40851–8

Liu JF, Zhang YM, Yi CX, Sun JM, Li WW (2004) [The expression and interaction of cyclin D1 and p16 in fibroblasts of pathologic scars]. *Zhonghua Zheng Xing Wai Ke Za Zhi* 20:265–7

Lorenzini A, Tresini M, Mawal-Dewan M, Frisoni L, Zhang H, Allen RG *et al.* (2002) Role of the Raf/MEK/ERK and the PI3K/Akt(PKB) pathways in fibroblast senescence. *Exp Gerontol* 37:1149–56

Luo S, Benathan M, Raffoul W, Panizzon RG, Egloff DV (2001) Abnormal balance between proliferation and apoptotic cell death in fibroblasts derived from keloid lesions. *Plast Reconstr Surg* 107:87–96

Marneros AG, Krieg T (2004) Keloids—clinical diagnosis, pathogenesis, and treatment options. *J Dtsch Dermatol Ges* 2:905–13

Masuda M, Suzui M, Lim JT, Deguchi A, Soh JW, Weinstein IB (2002) Epigallocatechin-3-gallate decreases VEGF production in head and neck and breast carcinoma cells by inhibiting EGFR-related pathways of signal transduction. *J Exp Ther Oncol* 2:350–9

Mirza AM, Kohn AD, Roth RA, McMahon M (2000) Oncogenic transformation of cells by a conditionally active form of the protein kinase Akt/PKB. *Cell Growth Differ* 11:279–92

Mutalik S (2005) Treatment of keloids and hypertrophic scars. *Indian J Dermatol Venereol Leprol* 71:3–8

Nowak KC, McCormack M, Koch RJ (2000) The effect of superpulsed carbon dioxide laser energy on keloid and normal dermal fibroblast secretion of growth factors: a serum-free study. *Plast Reconstr Surg* 105: 2039–48

Paul B, Hayes CS, Kim A, Athar M, Gilmour SK (2005) Elevated polyamines lead to selective induction of apoptosis and inhibition of tumorigenesis by (−)-epigallocatechin-3-gallate (EGCG) in ODC/Ras transgenic mice. *Carcinogenesis* 26:119–24

Phan TT, Lim IJ, Aalami O, Lorget F, Khoo A, Tan EK *et al.* (2005) Smad3 signalling plays an important role in keloid pathogenesis via epithelial–mesenchymal interactions. *J Pathol* 207:232–42

Phan TT, Lim IJ, Chan SY, Tan EK, Lee ST, Longaker MT (2004) Suppression of transforming growth factor beta/smad signaling in keloid-derived fibroblasts by quercetin: implications for the treatment of excessive scars. *J Trauma* 57:1032–7

Rekha A (2004) Keloids—a frustrating hurdle in wound healing. *Int Wound J* 1:145–8

Sah JF, Balasubramanian S, Eckert RL, Rorke EA (2004) Epigallocatechin-3-gallate inhibits epidermal growth factor receptor signaling pathway. Evidence for direct inhibition of ERK1/2 and AKT kinases. *J Biol Chem* 279:12755–62

Satish L, Babu M, Tran KT, Hebda PA, Wells A (2004) Keloid fibroblast responsiveness to epidermal growth factor and activation of downstream intracellular signaling pathways. *Wound Repair Regen* 12:183–92

Sato M (2006) Upregulation of the Wnt/beta-catenin pathway induced by transforming growth factor-beta in hypertrophic scars and keloids. *Acta Derm Venereol* 86:300–7

Surh YJ, Chun KS, Cha HH, Han SS, Keum YS, Park KK *et al.* (2001) Molecular mechanisms underlying chemopreventive activities of anti-inflammatory phytochemicals: down-regulation of COX-2 and iNOS through suppression of NF-kappa B activation. *Mutat Res* 480–481:243–68

Tan EM, Qin H, Kennedy SH, Rouda S, Fox JW 4th, Moore JH Jr (1995) Platelet-derived growth factors-AA and -BB regulate collagen and collagenase gene expression differentially in human fibroblasts. *Biochem J* 310(Part 2):585–8

Ullmann U, Haller J, Decourt JP, Girault N, Girault J, Richard-Caudron AS *et al.* (2003) A single ascending dose study of epigallocatechin gallate in healthy volunteers. *J Int Med Res* 31:88–101

Wang YC, Bachrach U (2002) The specific anti-cancer activity of green tea (−)-epigallocatechin-3-gallate (EGCG). *Amino Acids* 22:131–43

Wang Z, Ge L, Wang M, Carr BI (2006) Phosphorylation regulates Myc expression via prolonged activation of the mitogen-activated protein kinase pathway. *J Cell Physiol* 208:133–40

Wu WS, Wang FS, Yang KD, Huang CC, Kuo YR (2006) Dexamethasone induction of keloid regression through effective suppression of VEGF expression and keloid fibroblast proliferation. *J Invest Dermatol* 126: 1264–71

Wu Y, Zhang Q, Ann DK, Akhondzadeh A, Duong HS, Messadi DV *et al.* (2004) Increased vascular endothelial growth factor may account for elevated level of plasminogen activator inhibitor-1 via activating ERK1/2 in keloid fibroblasts. *Am J Physiol Cell Physiol* 286: C905–12

Xia W, Longaker MT, Yang GP (2006) P38 MAP kinase mediates transforming growth factor-beta2 transcription in human keloid fibroblasts. *Am J Physiol Regul Integr Comp Physiol* 290:R501–8

Yamamoto M, Tsukada S, Inoue M (1982) Possible age-associated change at cellular level in cultured fibroblasts derived from scar tissue. *Chirurgia Plastica* 7:51–8

You S, Moon JH, Kim TK, Kim SC, Kim JW, Yoon DH *et al.* (2004) Cellular characteristics of primary and immortal canine embryonic fibroblast cells. *Exp Mol Med* 36:325–35

Zhang Q, Wu Y, Chau CH, Ann DK, Bertolami CN, Le AD (2004) Crosstalk of hypoxia-mediated signaling pathways in upregulating plasminogen activator inhibitor-1 expression in keloid fibroblasts. *J Cell Physiol* 199:89–97

Zhu BH, Zhan WH, Li ZR, Wang Z, He YL, Peng JS *et al.* (2007) (−)-Epigallocatechin-3-gallate inhibits growth of gastric cancer by reducing VEGF production and angiogenesis. *World J Gastroenterol* 13: 1162–9